2023 62nd IEEE Conference on Decision and Control (CDC)
December 13-15, 2023. Marina Bay Sands, Singapore

Notch filter design with stability guarantees for mechanical resonance suppression in SISO LTI two-mass drive systems

Giulia Sonzogni, Mirko Mazzoleni, Marco Polver, Antonio Ferramosca and Fabio Previdi

Abstract— **Although the suppression of mechanical resonances for drive and positioning systems is a well-understood problem in the literature, its importance is still actual as technological developments push towards an increase in performance requirements. In this paper, the design of a notch filter is investigated with the aim of suppressing a single resonant frequency in SISO LTI two-mass drive systems. In the cases where the notch filter is located inside an existing control loop, as assumed in this work, it must not compromise the closed-loop stability of the system, while assuring desired control bandwidth and stability margins. Given a fixed known resonant frequency to suppress, an automatic algorithm is proposed to tune the notch filter parameters to guarantee specified control requirements and stability of the closed-loop system, so as to avoid, whenever possible, the reconfiguration of a preexisting controller.**

I. INTRODUCTION

Industry requirements demand fast accelerations and positioning accuracy of motion systems, and standard control tuning guidelines exist when the mechanical design is such that the system to be controlled is stiff and highly reproducible [1]. However, fast accelerations are facilitated by lightweight mechanical structures, that are often flexible [2]. On the other hand, the growing control performance requirements ask for the increase of the control bandwidth, with consequent shift of the flexible dynamics in the crossover control region [3]. The presence of flexible dynamics generally limits the achievable feedback control bandwidth, as unwanted oscillations and even instability may occur [4].

The management of flexible dynamics with both motor and load-side speed measurements is a well-known problem in motion control [3], [5], [6]. Additionally, motion control of two-mass systems is widely performed with PI/PID controllers [7], [8]. In this setting, one of the most common solutions to deal with a flexible mode in the control bandwidth (without decreasing the PI/PID controller gain or redesigning the system mechanics, as done in [9] and [10]) is the use of a notch filter centered at that single resonant frequency, with attenuation gain and filter bandwidth to be designed [1, Chapter 4]. The notch filter can be inserted both as a feedforward action, by filtering the reference signal, or inside the control loop if a positive phase contribution is needed. Notably, this latter design is the only viable solution when the reference signal is zero, as for stabilized servo-systems that must withstand external disturbances to keep their fixed constant position. Nonetheless, the insertion of a filter in an already-designed control loop should cause as few alterations as possible to the existing controller, so as not to compromise the control performance and closed-loop system stability.

Several approaches have been proposed to design a notch filter, also by adaptively estimating the resonance frequency to suppress [7], [11], [12], [13]. However, these approaches focused mainly on improving the goodness and computational complexity of the estimate of the resonant frequency, without directly assessing the stability of the closed-loop system after the insertion of the notch filter inside the control loop.

In this paper, an automatic algorithm is proposed to design a notch filter inside the speed control-loop for motion control systems, that guarantees under stated assumptions the asymptotic stability of the resulting closed loop, with the fewest possible alterations on control performance. It is considered a two-mass SISO LTI drive system with elastic transmission, with known transfer function and resonance frequency, controlled in velocity by a PI regulator with load-side speed measurement. The proposed algorithm needs only the parameters of the servo system and the PI controller coefficients in order to tune the notch filter, along with understandable configuration requirements specified by the user. The approach allows faster development of the motion control software without compromising a preexisting stabilizing controller.

II. PROBLEM STATEMENT

A. Two-mass drive system description

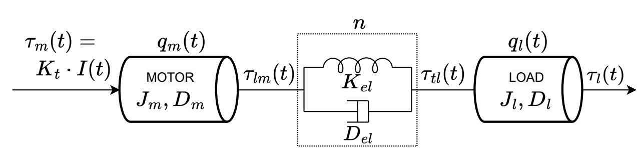

Fig. 1. Two-masses drive system with elastic coupling.

Consider the two-mass drive system with elastic coupling depicted in Fig. 1. Motor-side quantities are denoted by motor position $q_m(t)$, torque $\tau_m(t)$, inertia J_m and coefficient of viscous friction D_m. Load-side quantities are denoted by load position $q_l(t)$, torque $\tau_l(t)$, inertia J_l and coefficient of viscous friction D_l. The elastic coupling is modelled by a torsional spring with constant K_{el} and a damper with damping coefficient D_{el}. The transmission ratio is defined as $n = {\tau_{tl}(t)}/{\tau_{lm}(t)}$, where $\tau_{tl}(t)$ is the transmission output (load-side) torque and $\tau_{lm}(t)$ is the transmission input (motor-side) torque generated by the motor. The system in

G. Sonzogni, M. Mazzoleni, M. Polver, A. Ferramosca and F. Previdi are with the Department of Management, Information and Production Engineering, University of Bergamo, Via G. Marconi 5, 24044 Dalmine (BG), Italy. giulia.sonzogni@unibg.it

979-8-3503-0123-6/23/$31.00 ©2023 IEEE

Fig. 1 can thus be described by

$$\tau_m(t) = K_t \cdot I(t) \tag{1a}$$
$$J_m\ddot{q}_m(t) + D_m\dot{q}_m(t) = \tau_m(t) - \tau_{lm}(t) \tag{1b}$$
$$J_l\ddot{q}_l(t) + D_l\dot{q}_l(t) = \tau_{tl}(t) - \tau_l(t) \tag{1c}$$
$$\tau_{lm}(t) = K_{el}(q_m(t) - nq_l(t)) + D_{el}(\dot{q}_m(t) - n\dot{q}_l(t)) \tag{1d}$$

where K_t is the motor torque constant and $I(t)$ is the motor torque-generating current. Let $\tau_l = D_m = D_l = 0$. The transfer function $G_{vl}(s)$ from motor current $I(t)$ to load speed (referred to the motor shaft) $n \cdot \dot{q}_l(t)$ reads as

$$G_{vl}(s) = \frac{\tilde{\Omega}_l(s)}{I(s)} = n\frac{\Omega_l(s)}{I(s)} = \frac{\mu}{s}\frac{1 + 2\dfrac{\xi_z}{\omega_z}s}{1 + 2\dfrac{\xi_p}{\omega_p}s + \dfrac{s^2}{\omega_p^2}}, \tag{2}$$

where $I(s), \Omega_m(s), \Omega_l(s)$ are the Laplace transformed motor current, motor rotation speed and load rotation speed, $\tilde{\Omega}_l(s)$ is the load rotation speed referred to the motor shaft, ω_z, ω_p are the zeros/poles resonance frequencies and ξ_z, ξ_p are the zeros/poles damping coefficients.

It is considered a speed closed-loop system for $G_{vl}(s)$ in (2) with load-side velocity measurement $\dot{q}_l(t)$, as shown in Fig. 2. The controller $R(s)$ is assumed to be a Proportional-Integral (PI) one, with proportional gain $K_p > 0$ and integral gain $K_i > 0$. The speed loop transfer function $L(s)$ reads as

$$L(s) = R(s)G_{vl}(s) = \left(K_p + \frac{K_i}{s}\right)\frac{\mu}{s}\frac{1 + 2\dfrac{\xi_z}{\omega_z}s}{1 + 2\dfrac{\xi_p}{\omega_p}s + \dfrac{s^2}{\omega_p^2}}. \tag{3}$$

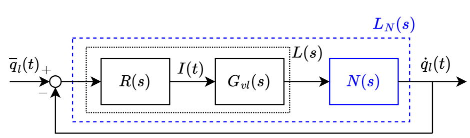

Fig. 2. Loop transfer function $L(s)$ with PI controller $R(s)$ for the system $G_{vl}(s)$ in (2) with load-side speed measurement. When a notch filter $N(s)$ is inserted in the loop, the loop function becomes $L_N(s)$.

The transfer function in (3) might present a resonance peak at ω_p with magnitude greater than 0_{dB}, which can cause unwanted vibrations in the load speed output $\dot{q}_l(t)$ as in Fig. 3. Notice how in these cases the magnitude of $L(s)$ intersects the 0_{dB} axis more than once (specifically, 3 times).

Two common definitions are now stated for later use. [14]

Definition 1 (Gain crossover frequency): The *gain crossover frequency* ω_c of an open-loop transfer function $L(s)$ is the lowest frequency at which the magnitude of $L(s)$ intersects the 0_{dB} axis, that is

$$\omega_c : \quad |L(j\omega_c)|_{\text{dB}} = 0_{\text{dB}}. \tag{4}$$

Definition 2 (Phase margin): The *phase margin* φ_m is the number of degrees by which the phase angle of $L(s)$ is smaller than $-180°$ at the gain crossover frequency, that is

$$\varphi_m := 180° - |\varphi_c|, \quad \varphi_c := \angle\, L(j\omega_c). \tag{5}$$

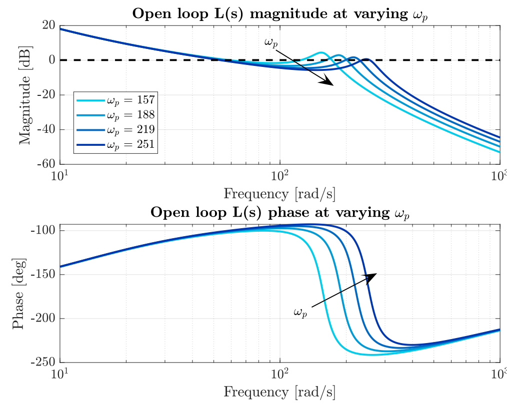

Fig. 3. Bode diagram of $L(s)$ at varying resonance frequency ω_p, $\omega_z = 80.27$ [rad/s], $\xi_p = 0.1$, $\xi_z = 0.058$, $K_p = 0.2342$,$K_i = 2.9269$.

B. Notch filter description

A classical solution to suppress the resonance peak at frequency ω_p in (3) is to use a notch filter $N(s)$

$$N(s) = \frac{1 + 2\dfrac{\xi_1}{\omega_n}s + \dfrac{s^2}{\omega_n^2}}{1 + 2\dfrac{\xi_2}{\omega_n}s + \dfrac{s^2}{\omega_n^2}}, \tag{6}$$

where the notched frequency ω_n and the zeros/poles dampings $0 < \xi_1 < 1, 0 < \xi_2 < 1$ are *design parameters*. A standard tuning is

$$\omega_n = \omega_p, \qquad \xi_1 = \xi_p, \tag{7}$$

with $\xi_p \ll \xi_2$ so to substitute the resonant poles with damped ones. With this rationale, the design freedom is left only to the parameter ξ_2. Applying (6)-(7) to (3) leads to a new loop function $L_N(s) = L(s)N(s)$, see Fig. 2:

$$L_N(s) = \left(K_p + \frac{K_i}{s}\right)\frac{\mu}{s}\frac{1 + 2\dfrac{\xi_z}{\omega_z}s}{1 + 2\dfrac{\xi_2}{\omega_p}s + \dfrac{s^2}{\omega_p^2}}. \tag{8}$$

The gain crossover frequency of (8) follows from Definition 1 as

$$\omega_{c,N} : \quad |L_N(j\omega_{c,N})|_{\text{dB}} = 0_{\text{dB}}, \tag{9}$$

and the *phase margin* φ_N follows from Definition 2 as

$$\varphi_N := 180° - |\varphi_{c,N}|, \quad \varphi_{c,N} := \angle\, L_N(j\omega_{c,N}). \tag{10}$$

The aim of this paper is to *automatically design* the parameter ξ_2 of a notch filter $N(s)$ in (6) with initial configuration as in (7) to suppress the resonant peak of $L(s)$ in (3), so that the resulting loop function $L_N(s)$ in (8) maintains a phase margin $\varphi_N > \bar{\varphi}$, with $\bar{\varphi}$ chosen by the designer, and approximately the same bandwidth of $L(s)$, that is $\omega_{c,N} \approx \omega_c$. Under the validity of the Bode's stability criterion, a positive gain of $L_N(s)$ and a positive phase margin φ_N in (10) ensure the asymptotic stability of the feedback system $F_N(s) = L_N(s)/(1 + L_N(s))$. The proposed approach assumes the knowledge of (3) and explicitly avoids any computation on (8) to allow a fast algorithm with simple implementation.

III. Automatic notch filter design

This section first analyses the frequency response of the the notch filter (6) - (7), highlighting a tradeoff between notch magnitude and bandwidth when setting ξ_2. Based on this, an automatic design strategy for ξ_2 is proposed.

Let $N(s)$ be a notch filter as in (6) - (7), with $\xi_1 < \xi_2$. The gain of $N(s)$ at frequency ω_n is *inversely proportional* to ξ_2

$$|N(j\omega_n)|_{\text{dB}} = 20\log_{10}\frac{\xi_1}{\xi_2}. \tag{11}$$

Conversely, the notch filter stop-bandwidth[1] is *directly proportional* to ξ_2, as empirically shown in Fig. 4. The effect

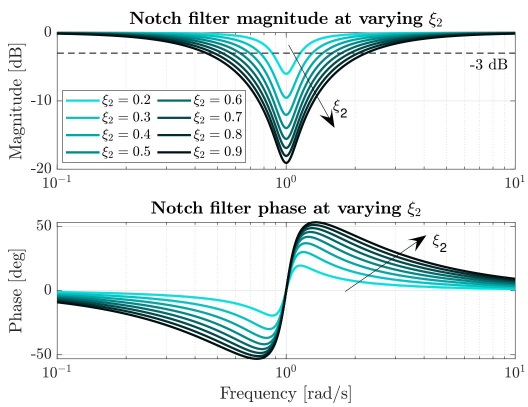

Fig. 4. Notch filter Bode diagrams at varying ξ_2, with $\xi_1 = 0.1$ and $\omega_n = 1$ rad/s. The arrow denotes increasing values of ξ_2.

of ξ_2 on the notch magnitude and stop-bandwidth highlights a *tradeoff* in the choice of ξ_2: a high ξ_2 value leads to a high notch attenuation at ω_n, with corresponding increase of the notch stop-bandwidth. Thus, increasing ξ_2 may decrease $\omega_{c,N}$ in (9). This aspect is considered next in the proposed automatic design of ξ_2.

The design strategy relies on the following assumptions:

- **A1)** The magnitude of $L(s)$ in (3) intersects 0_{dB} more than once, as shown in Fig. 3;
- **A2)** The resonance frequency ω_p is such that $\omega_p > \omega_c$;
- **A3)** The notch filter $N(s)$ is defined as in (6) - (7) with $\xi_1 < \xi_2$.

Assumption **A1)** is common in drive systems and it is the starting point of this work. To verify this assumption, (4) can be efficiently solved for ω_c as shown in the appendix. The gain crossover frequency (4) of (3) is the solution with the lowest positive value. Assumption **A2)** derives from common mechatronics control design.

For the proposed tuning strategy, the control designer has to set the following design parameters, which in turn define two constraints on the notch filter design:

- **C1)** The *minimum (negative) value of notch filter gain* $\bar{M}_{\text{dB}} < 0$ at the gain crossover frequency ω_c in (4), so that
$$|N(j\omega_c)|_{\text{dB}} \geq \bar{M}_{\text{dB}}. \tag{12}$$
The constraint (12) imposes also a limit on the bandwidth of $N(s)$, so not to interfere with the magnitude of $L_N(s)$ in the neighbourhoods of ω_c, to enforce $\omega_{c,N} \approx \omega_c$.
- **C2)** The *minimum phase margin* $\bar{\varphi} > 0$ of $L_N(s)$ in (10), so that
$$\varphi_N \geq \bar{\varphi} > 0. \tag{13}$$
Under the validity of the Bode's stability criterion, this guarantees that $F_N(s) = L_N(s)/(1 + L_N(s))$ is asymptotically stable.

[1] Defined as the frequency range that lies under the -3dB axis.

A. Design of ξ_2 for constraint C1)

From Assumption **A3)**, the notch magnitude is negative, see Fig.4. The insertion of the notch in the loop will reduce the magnitude of $L(s)$ with the possibility to modify the bandwidth of $L_N(s)$, with the consequence that $\omega_{c,N} \leq \omega_c$.

Proposition 1: Under **A1)-A3)**, given $\bar{M}_{\text{dB}} < 0$, the constraint (12) holds for every value of ξ_2 so that

$$0 < \xi_2 \leq \tilde{\xi}, \tag{14}$$

where

$$\tilde{\xi} := \sqrt{\frac{\left(\omega_n^2 - \omega_c^2\right)^2 + 4\xi_1^2\omega_n^2\omega_c^2 - 10^{\bar{M}_{\text{dB}}/10}\cdot\left(\omega_n^2 - \omega_c^2\right)^2}{4\omega_n^2\omega_c^2 \cdot 10^{\bar{M}_{\text{dB}}/10}}} \tag{15}$$

Proof: The proof is in the appendix. ∎

B. Design ξ_2 for constraint C2)

To satisfy the constraint in (13), the notch filter has to be designed so that

$$180° - |\angle L(j\omega_{c,N}) + \angle N(j\omega_{c,N})| \geq \bar{\varphi} > 0. \tag{16}$$

Under **A2)-A3)**, it is true that $\angle N(j\omega_c) < 0°$. Thus, since $\omega_{c,N} \leq \omega_c$, it follows that $\angle N(j\omega_{c,N}) < 0°$. So, the application of $N(s)$ in (6) to $L(s)$ in (3) will lead to $\varphi_N \leq \varphi_m$, see also Fig. 4. Considering (3), it is true that

$$\angle L(j\omega) < 0°, \quad \forall\omega. \tag{17}$$

Thus,

$$|\angle L(j\omega_{c,N}) + \angle N(j\omega_{c,N})| = |\angle L(j\omega_{c,N})| + |\angle N(j\omega_{c,N})|,$$

and (16) reads as

$$-|\angle N(j\omega_{c,N})| \geq \bar{\varphi} - 180° + |\angle L(j\omega_{c,N})| \tag{18a}$$
$$\angle N(j\omega_{c,N}) \geq -\big(180° - |\angle L(j\omega_{c,N})| - \bar{\varphi}\big), \tag{18b}$$

where (18b) follows from the fact that $\angle N(j\omega_{c,N}) < 0°$. Define $\bar{\theta} := \big(180° - |\angle L(j\omega_c)| - \bar{\varphi}\big)$. Then, the following proposition holds.

Proposition 2: Under **A1)-A3)** and assuming further that

$$\left(2\omega_n \cdot \omega_{c,N}\left(\omega_n^2 - \omega_{c,N}^2\right) + \tan\left(-\bar{\theta}\right) 4\xi_1\omega_{c,N}^2\omega_n^2\right) > 0,$$

given a $\bar{\varphi} > 0$, the constraint (13) holds for every value of ξ_2 when

$$0 < \xi_2 \leq \bar{\xi}, \tag{19}$$

where

$$\bar{\xi} := \frac{2\xi_1\omega_n \cdot \omega_{c,N}\left(\omega_n^2 - \omega_{c,N}^2\right) - \tan\left(-\bar{\theta}\right) \cdot \left(\omega_n^2 - \omega_{c,N}^2\right)^2}{2\omega_n \cdot \omega_{c,N}\left(\omega_n^2 - \omega_{c,N}^2\right) + \tan\left(-\bar{\theta}\right) 4\xi_1\omega_{c,N}^2 \cdot \omega_n^2} \tag{20}$$

Proof: The proof is in the appendix. ■

Thus, ξ_2 should be chosen such that

$$0 < \xi_2 \leq \min\left(\bar{\xi}, \widetilde{\xi}, 1\right). \tag{21}$$

C. Design of the notch filter attenuation gain

The choice of ξ_2 highlights a *tradeoff* between:

1) the constraint (21) (lower ξ_2);
2) the gain of the notch filter at ω_p (higher ξ_2), so that

$$|L_N(j\omega_p)|_{\mathrm{dB}} < 0, \tag{22}$$

in order to damp the resonance at ω_p (that is the primary application of the notch filter in this work).

The condition (22) guarantees that the magnitude of $L_N(s)$ intersects 0_{dB} axis only once and so the existence of one unique gain crossover frequency $\omega_{c,N}$. The satisfaction of (22) and stable poles[2] in $L_N(s)$ allows the application of the Bode's stability theorem. A positive phase margin φ_N, ensured by (13), and a positive gain[3] of $L_N(s)$ guarantee the stability of $F_N(s)$. Considering $\bar{\xi} < 1$ and $\widetilde{\xi} < 1$, an automatic rule to set ξ_2 is thus

$$\xi_2 = \min(\bar{\xi}, \widetilde{\xi}). \tag{23}$$

The limits in (15) and (20) depend heavily from the parameters $\bar{M}_{\mathrm{dB}}$ and $\bar{\varphi}$ in (12)-(13) chosen by the designer. In particular, if $\bar{\varphi} > \varphi_m$, it is not possible to choose a value for ξ_2 that respects (15), (20) and (22). As a result of this, it is recommended to choose a *minimum phase margin* $\bar{\varphi}$ considering φ_m, for instance by setting

$$\bar{\varphi} = \alpha \cdot \varphi_m, \quad 0 < \alpha < 1. \tag{24}$$

A summary is presented in Algorithm 1.

IV. Simulations and Result

In order to verify the effectiveness of the proposed method for tuning the parameter ξ_2 of (6), a simulated system as in (3) is considered, where: $J_l = 6.7$ [Kg m^2], $J_m = 4.77 \cdot 10^{-5}$ [Kg m^2], $n = 266$, $K_t = 0.0304$ [Nm/A], $\omega_z = 80.27$ [rad/s], $\omega_p = 138.23$ [rad/s], $\xi_z = 0.0581$, $\xi_p = 0.1$, $K_p = 0.2342$, $K_i = 2.9269$. Since it is assumed that $\omega_{c,N}$ in (9) is not known as its computation is cumbersome, the practical computation of (20) can be performed by using ω_c in (4) in place of $\omega_{c,N}$. This substitution is motivated by (12).

Fig. 5 shows a case where $\bar{M}_{\mathrm{dB}} = -1_{\mathrm{dB}}$ and $\alpha = 80\%$, so the *minimum phase margin* is set to $\bar{\varphi} \approx 62°$. After the application of $N(s)$, tuned with Algorithm 1, the phase margin of $L_N(s)$ results $\varphi_N \approx 63°$. In this case the constraint **C2)** is more restrictive than the constraint **C1)**, in fact $\bar{\xi} = 0.3393$ and $\widetilde{\xi} = 0.4320$. The algorithm sets $\xi_2 = \min\left(\bar{\xi}, \widetilde{\xi}\right) = 0.3393$ according to (23) so the inequality in (13) becomes an equation and it's correct to obtain $\varphi_N \approx \bar{\varphi}$.

[2] For $0 < \xi_2 < 1$ the poles of $L_N(s)$ are stable.

[3] The gain of $L_N(s)$ is $\mu K_i > 0$ by the physical properties of the system (2) and by the positive controller gains K_p in $R(s)$.

Algorithm 1 Automatic tuning ξ_2

Input: α, $\bar{M}_{\mathrm{dB}}$, $L(s)$, ω_n, ξ_1

x = solutions of (4)
if (the number of solutions x in greater than one) **then**
  $\omega_c = \min(x)$ s.t. $x > 0$
  $\bar{\varphi} = \alpha \cdot |\angle L(j\omega_c)|$ as in (24)
  $\bar{\theta} = 180° - |\angle L(j\omega_c)| - \bar{\varphi}$
  Compute $\widetilde{\xi}$ as in (15)
  Compute $\bar{\xi}$ as in (20)
  $\xi_2 = \min(\widetilde{\xi}, \bar{\xi})$ as in (23)
  if ($\xi_2 > 0$ **and** $\xi_2 < 1$ **and** $|L_N(j\omega_p)|_{\mathrm{dB}} < 0$) **then**
    A value ξ_2 that satisfies (21)-(22) has been found.
  else
    No value ξ_2 that satisfies (21)-(22) has been found. The constraint C1) or C2) is too restrictive.
  end if
end if

Output: tuned ξ_2

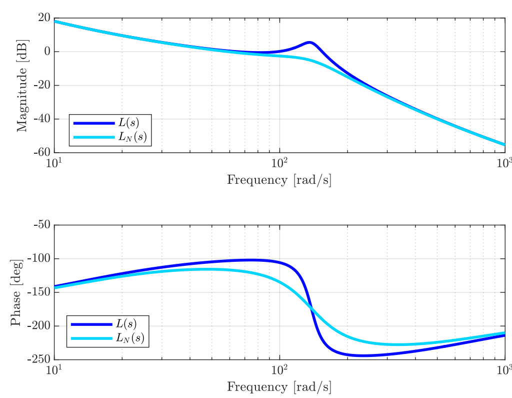

Fig. 5. Open loop functions $L(s)$ and $L_N(s)$. Bode diagrams at $\omega_p = 138.23$ [rad/s]

The same servomechanism has been tested with different values of α and fixed $\bar{M}_{\mathrm{dB}} = -1_{\mathrm{dB}}$ with the aim of analysing how the ξ_2 parameter, the gain crossover frequency $\omega_{c,N}$ and the phase margin φ_N vary. The results are shown in Tab. I. As α decreases, constraint **C1)** becomes less restrictive and the tuned ξ_2 increases, until constraint **C2)** intervenes. In fact, for $\alpha = 70\%$ and $\alpha = 60\%$, the ξ_2 value is the same, since it is limited by the value of $\bar{M}_{\mathrm{dB}} = -1_{\mathrm{dB}}$.

α	85%	80%	75%	70%	60%
ω_p [rad/s]	138.23	138.23	138.23	138.23	138.23
ω_c [rad/s]	65.9	65.9	65.9	65.9	65.9
$\bar{\varphi}$ [°]	≈ 66	≈ 62	≈ 58	≈ 54	≈ 46.5
ξ_2	0.2759	0.3393	0.4064	0.4320	0.4320
$\omega_{c,N}$ [rad/s]	61	59.3	57.6	56.9	56.9
φ_N [°]	≈ 67	≈ 63	≈ 60	≈ 59	≈ 59

TABLE I
RESULTS WITH DIFFERENT α VALUES.

The algorithm has been tested also with fixed $\alpha = 0.8$ and different values of $\bar{M}_{\mathrm{dB}}$; the results are shown in Tab.

$\bar{M}_{\text{dB}}$	-1	-0.8	-0.6	-0.3
ω_p [rad/s]	138.23	138.23	138.23	138.23
ω_c [rad/s]	65.9	65.9	65.9	65.9
$\bar{\varphi}$ [°]	≈ 62	≈ 62	≈ 62	≈ 62
ξ_2	0.3393	0.3393	0.3333	0.2425
$\omega_{c,N}$ [rad/s]	59.3	59.3	59.5	61.9
φ_N [°]	≈ 63	≈ 63	≈ 64	≈ 68

TABLE II

RESULTS WITH DIFFERENT $\bar{M}_{\text{DB}}$ VALUES.

II. As $\bar{M}_{\text{dB}}$ decreases, the ξ_2 value decreases and also the difference between the gain crossover frequency ω_c and the gain crossover frequency $\omega_{c,N}$ decreases. The ξ_2 value obtained by the algorithm when $\bar{M}_{\text{dB}} = -1_{\text{dB}}$ and $\bar{M}_{\text{dB}} = -0.8_{\text{dB}}$ is the same as in these cases the constraint **C2)** is more restrictive than the constraint **C1)**.

A low value of $\bar{M}_{\text{dB}}$ is necessary to keep $\omega_c \approx \omega_{c,N}$ and a high value of α is advisable to obtain a high φ_N. However, choosing a too-low value of $\bar{M}_{\text{dB}}$ and a too-high value of α is not recommended because this would lead to obtain a low ξ_2 value. When $|\xi_2| < 0.3$ the magnitude of $L_N(s)$ presents a peak at the poles' frequency. In these cases it is important that the peak is still less than 0_{dB}, as explained in section III-C.

The adaptability of the proposed algorithm has been tested by varying the ω_p value of the servomechanism and using as hyperparameters: $\bar{M}_{\text{dB}} = -1_{\text{dB}}$ and $\alpha = 80\%$. As shown in Tab. III, the effect produced by the resonance varies according to the poles resonant frequency.

ω_p [rad/s]	138.23	157	188.5	219.9
ξ_2	0.3393	0.4249	0.5377	0.6397
$\bar{\varphi}$ [°]	≈ 62.4	≈ 62	≈ 62.7	≈ 62.9
ω_c [rad/s]	65.9	59.9	56.4	54.8
$\omega_{c,N}$ [rad/s]	59.3	55.6	53.2	52
φ_N [°]	≈ 63	≈ 63	≈ 63	≈ 63

TABLE III

RESULTS WITH DIFFERENT ω_p VALUES.

In all simulations, it is possible to check that $\varphi_N \approx \bar{\varphi}$. In addition, since the conditions of the Bode's stability criterion are respected, a positive gain of $L_N(s)$ and a positive phase margin φ_N guarantee the asympotic stability of the resulting closed-loop system $F_N(s)$. The results obtained by the simulation demonstrate the capability to suppress the resonance at different frequencies, keeping a high control performance and guaranteeing a stable closed-loop system.

V. Conclusion

This paper presented an automatic method to tune a notch filter for suppressing the main resonance in two-drive mass systems, so as not to affect the system performance and guarantee the control loop stability after the notch application. The proposed approach is simple, allows a fast computation and needs only the configuration of two parameters. Furthermore, the effectiveness of the algorithm is shown in simulations under varying system configurations.

VI. Appendix

A. *Solving* (4) *in closed form*

Consider $L(s)$ in (3). The magnitude of $L(s)$ at a frequency ω reads as

$$|L(j\omega)|_{\text{dB}} = 20\log_{10}\left(\sqrt{K_p^2 + \frac{K_i^2}{\omega^2}}\frac{\mu}{\omega}\frac{\sqrt{1+\frac{4\xi_z^2\omega^2}{\omega_z^2}}}{\sqrt{\left(1-\frac{\omega^2}{\omega_p^2}\right)^2+\frac{4\xi_p^2\omega^2}{\omega_p^2}}}\right).$$

Solving (4) for a generic ω leads to the expression

$$\sqrt{K_p^2 + \frac{K_i^2}{\omega^2}}\frac{\mu}{\omega}\frac{\sqrt{1+\frac{4\xi_z^2\omega^2}{\omega_z^2}}}{\sqrt{\left(1-\frac{\omega^2}{\omega_p^2}\right)^2+\frac{4\xi_p^2\omega^2}{\omega_p^2}}} = 1,$$

$$\frac{\sqrt{K_p^2\omega^2+K_i^2}\,\mu\sqrt{1+\frac{4\xi_z^2\omega^2}{\omega_z^2}}-\omega^2\sqrt{\left(1-\frac{\omega^2}{\omega_p^2}\right)^2+\frac{4\xi_p^2\omega^2}{\omega_p^2}}}{\omega^2\sqrt{\left(1-\frac{\omega^2}{\omega_p^2}\right)^2+\frac{4\xi_p^2\omega^2}{\omega_p^2}}} = 0,$$

$$\left(-\frac{1}{\omega_p^4}\right)\omega^8 + \left(\frac{2}{\omega_p^2} - \frac{4\xi_p^2}{\omega_p^2}\right)\omega^6 + \left(\frac{4\mu^2\xi_z^2K_p^2}{\omega_z^2} - 1\right)\omega^4 + \\ + \left(K_p^2\mu^2 + \frac{4\mu^2\xi_z^2K_i^2}{\omega_z^2}\right)\omega^2 + \mu^2K_i^2 = 0.$$

Employing the substitution $t = \omega^2$, the associated quartic equation is achieved

$$\left(-\frac{1}{\omega_p^4}\right)t^4 + \left(\frac{2}{\omega_p^2} - \frac{4\xi_p^2}{\omega_p^2}\right)t^3 + \left(\frac{4\mu^2\xi_z^2K_p^2}{\omega_z^2} - 1\right)t^2 + \\ + \left(K_p^2\mu^2 + \frac{4\mu^2\xi_z^2K_i^2}{\omega_z^2}\right)t + \mu^2K_i^2 = 0. \tag{25}$$

The solutions of (4) are the positive roots of (25), that is $\omega_1 = \sqrt{t_1}, \omega_2 = \sqrt{t_2}, \omega_3 = \sqrt{t_3}, \omega_4 = \sqrt{t_4}$, where t_1, t_2, t_3, t_4 are positive and real.

B. *Proof of proposition 1*

The magnitude of the notch filter frequency response at frequency ω_c reads as

$$|N(j\omega_c)| = \frac{\sqrt{\left(\omega_n^2-\omega_c^2\right)^2+4\xi_1^2\omega_n^2\omega_c^2}}{\sqrt{\left(\omega_n^2-\omega_c^2\right)^2+4\xi_2^2\omega_n^2\omega_c^2}} \tag{26}$$

so that constraint (12) can be rewritten as

$$|N(j\omega_c)| = \frac{\sqrt{\left(\omega_n^2-\omega_c^2\right)^2+4\xi_1^2\omega_n^2\omega_c^2}}{\sqrt{\left(\omega_n^2-\omega_c^2\right)^2+4\xi_2^2\omega_n^2\omega_c^2}} \geq 10^{\frac{\bar{M}_{\text{dB}}}{20}}, \tag{27}$$

$$\frac{\sqrt{(\omega_n^2-\omega_c^2)^2+4\xi_1^2\omega_n^2\omega_c^2}-10^{\frac{\bar{M}_{\text{dB}}}{20}}\sqrt{(\omega_n^2-\omega_c^2)^2+4\xi_2^2\omega_n^2\omega_c^2}}{\sqrt{(\omega_n^2-\omega_c^2)^2+4\xi_2^2\omega_n^2\omega_c^2}} \geq 0. \tag{28}$$

The denominator of (28) is always greater than zero. Thus, it is necessary to study the sign of the numerator of (28) to assess when (28) holds true.

$$\sqrt{(\omega_n^2-\omega_c^2)^2+4\xi_1^2\omega_n^2\omega_c^2} - 10^{\frac{\bar{M}_{\text{dB}}}{20}}\sqrt{(\omega_n^2-\omega_c^2)^2+4\xi_2^2\omega_n^2\omega_c^2} \geq 0$$

$$\sqrt{\left(\omega_n^2-\omega_c^2\right)^2+4\xi_1^2\omega_n^2\omega_c^2} \geq 10^{\frac{\bar{M}_{\mathrm{dB}}}{20}}\sqrt{\left(\omega_n^2-\omega_c^2\right)^2+4\xi_2^2\omega_n^2\omega_c^2}$$

$$\left(\omega_n^2-\omega_c^2\right)^2+4\xi_1^2\omega_n^2\omega_c^2 \geq 10^{\frac{\bar{M}_{\mathrm{dB}}}{20}}\left(\left(\omega_n^2-\omega_c^2\right)^2+4\xi_2^2\omega_n^2\omega_c^2\right)$$

$$\left(\omega_n^2-\omega_c^2\right)^2+4\xi_1^2\omega_n^2\omega_c^2 \geq 10^{\frac{2\bar{M}_{\mathrm{dB}}}{20}}\left(\omega_n^2-\omega_c^2\right)^2+10^{\frac{2\bar{M}_{\mathrm{dB}}}{20}}\left(4\xi_2^2\omega_n^2\omega_c^2\right)$$

$$\xi_2^2 \leq \frac{\left(\omega_n^2-\omega_c^2\right)^2+4\xi_1^2\omega_n^2\omega_c^2-10^{\frac{\bar{M}_{\mathrm{dB}}}{10}}\left(\omega_n^2-\omega_c^2\right)^2}{4\omega_n^2\omega_c^2\cdot 10^{\frac{\bar{M}_{\mathrm{dB}}}{10}}} \tag{29}$$

It is possible to notice that

$$10^{\frac{\bar{M}_{\mathrm{dB}}}{10}} < 1,$$

due to the fact that $\bar{M}_{\mathrm{dB}} < 0$. It follows that

$$\left(\omega_n^2-\omega_c^2\right)^2-10^{\frac{\bar{M}_{\mathrm{dB}}}{10}}\cdot\left(\omega_n^2-\omega_c^2\right)^2 \geq 0,$$

and thus the numerator of (29) is not negative.

Thus, an upper bound can be computed for ξ_2 as

$$\widetilde{\xi}_2 := \sqrt{\frac{\left(\omega_n^2-\omega_c^2\right)^2+4\xi_1^2\omega_n^2\omega_c^2-10^{\frac{\bar{M}_{\mathrm{dB}}}{10}}\cdot\left(\omega_n^2-\omega_c^2\right)^2}{4\omega_n^2\omega_c^2\cdot 10^{\frac{\bar{M}_{\mathrm{dB}}}{10}}}} \tag{30}$$

C. Proof of Proposition 2

The frequency response of the notch filter in (6) at the frequency ω_c is

$$N(j\omega_{c,N}) = \frac{(j\omega_{c,N})^2+2\xi_1\omega_n\cdot j\omega_{c,N}+\omega_n^2}{(j\omega_{c,N})^2+2\xi_2\omega_n\cdot j\omega_{c,N}+\omega_n^2}$$
$$= \frac{\left(\omega_n^2-\omega_{c,N}^2\right)+2\xi_1\omega_n\cdot j\omega_{c,N}}{\left(\omega_n^2-\omega_{c,N}^2\right)+2\xi_2\omega_n\cdot j\omega_{c,N}}\cdot\frac{\left(\omega_n^2-\omega_{c,N}^2\right)-2\xi_2\omega_n\cdot j\omega_{c,N}}{\left(\omega_n^2-\omega_{c,N}^2\right)-2\xi_2\omega_n\cdot j\omega_{c,N}}$$

The real and imaginary parts follow as

$$\mathrm{Real}\left[N(j\omega_{c,N})\right] = \frac{\left(\omega_n^2-\omega_{c,N}^2\right)^2+4\xi_1\xi_2\omega_{c,N}^2\omega_n^2}{\left(\omega_n^2-\omega_{c,N}^2\right)^2+4\xi_2^2\omega_{c,N}^2\omega_n^2} \tag{31}$$

$$\begin{aligned}\mathrm{Img}\left[N(j\omega_{c,N})\right] = &\frac{2\xi_1\omega_n\cdot\omega_{c,N}\left(\omega_n^2-\omega_{c,N}^2\right)}{\left(\omega_n^2-\omega_{c,N}^2\right)^2+4\xi_2^2\omega_{c,N}^2\omega_n^2}+\\ &+\frac{-2\xi_2\omega_n\cdot\omega_{c,N}\left(\omega_n^2-\omega_{c,N}^2\right)}{\left(\omega_n^2-\omega_{c,N}^2\right)^2+4\xi_2^2\omega_{c,N}^2\omega_n^2}.\end{aligned} \tag{32}$$

Since $\mathrm{Real}\left[N(j\omega_{c,N})\right] > 0$ then

$$\angle N(j\omega_{c,N}) = \tan^{-1}\left(\frac{\mathrm{Img}\left[N(j\omega_{c,N})\right]}{\mathrm{Real}\left[N(j\omega_{c,N})\right]}\right). \tag{33}$$

The condition (18b) than reads as

$$\begin{aligned}\tan^{-1}\left(\frac{\mathrm{Img}\left[N(j\omega_{c,N})\right]}{\mathrm{Real}\left[N(j\omega_{c,N})\right]}\right) &\geq -\bar{\theta},\\ \frac{\mathrm{Img}\left[N(j\omega_{c,N})\right]}{\mathrm{Real}\left[N(j\omega_{c,N})\right]} &\geq \tan\left(-\bar{\theta}\right),\end{aligned} \tag{34}$$

$$\frac{2\xi_1\omega_n\cdot\omega_{c,N}\left(\omega_n^2-\omega_{c,N}^2\right)-2\xi_2\omega_n\cdot\omega_{c,N}\left(\omega_n^2-\omega_{c,N}^2\right)}{\left(\omega_n^2-\omega_{c,N}^2\right)^2+4\xi_1\xi_2\omega_{c,N}^2\omega_n^2} - \tan\left(-\bar{\theta}\right) \geq 0,$$

$$\frac{2\xi_1\omega_n\cdot\omega_{c,N}\left(\omega_n^2-\omega_{c,N}^2\right)-2\xi_2\omega_n\cdot\omega_{c,N}\left(\omega_n^2-\omega_{c,N}^2\right)}{\left(\omega_n^2-\omega_c^2\right)^2+4\xi_1\xi_2\omega_{c,N}^2\omega_n^2}+$$
$$+\frac{-\tan\left(-\bar{\theta}\right)\left(\omega_n^2-\omega_{c,N}^2\right)^2-\tan\left(-\bar{\theta}\right)4\xi_1\xi_2\omega_{c,N}^2\omega_n^2}{\left(\omega_n^2-\omega_{c,N}^2\right)^2+4\xi_1\xi_2\omega_{c,N}^2\omega_n^2} \geq 0. \tag{35}$$

Since $\xi_2 > 0$ and $\xi_1 > 0$ by filter definition and $\omega_n = \omega_p > \omega_c \approx \omega_{c,N}$, the denominator of (35) is always greater than zero. The numerator of (35) is ≥ 0 when

$$\xi_2\cdot\left(2\omega_n\cdot\omega_{c,N}\left(\omega_n^2-\omega_{c,N}^2\right)+\tan\left(-\bar{\theta}\right)4\xi_1\omega_{c,N}^2\omega_n^2\right) <$$
$$\leq 2\xi_1\omega_n\cdot\omega_{c,N}\left(\omega_n^2-\omega_{c,N}^2\right)-\tan\left(-\bar{\theta}\right)\cdot\left(\omega_n^2-\omega_{c,N}^2\right)^2.$$

By assuming that

$$\left(2\omega_n\cdot\omega_{c,N}\left(\omega_n^2-\omega_{c,N}^2\right)+\tan\left(-\bar{\theta}\right)4\xi_1\omega_{c,N}^2\omega_n^2\right) > 0,$$

it's possible set an upper bound for ξ_2 as

$$\xi_2 \leq \frac{2\xi_1\omega_n\cdot\omega_{c,N}\left(\omega_n^2-\omega_{c,N}^2\right)-\tan\left(-\bar{\theta}\right)\cdot\left(\omega_n^2-\omega_{c,N}^2\right)^2}{2\omega_n\cdot\omega_{c,N}\left(\omega_n^2-\omega_{c,N}^2\right)+\tan\left(-\bar{\theta}\right)4\xi_1\omega_{c,N}^2\omega_n^2}.$$

References

[1] R. M. Schmidt, G. Schitter, and A. Rankers, *The design of high performance mechatronics: high-tech functionality by multidisciplinary system integration.* Ios Press, 2020.

[2] T. Oomen, "Advanced motion control for precision mechatronics: Control, identification, and learning of complex systems," *IEEJ Journal of Industry Applications*, vol. 7, no. 2, pp. 127–140, 2018.

[3] G. J. Balas and J. C. Doyle, "Control of lightly damped, flexible modes in the controller crossover region," *Journal of Guidance, Control, and Dynamics*, vol. 17, no. 2, pp. 370–377, 1994.

[4] M. Steinbuch and M. Norg, "Advanced motion control: An industrial perspective," *European Journal of Control*, vol. 4, no. 4, pp. 278–293, 1998.

[5] K. Ohnishi, M. Shibata, and T. Murakami, "Motion control for advanced mechatronics," *IEEE/ASME Transactions on Mechatronics*, vol. 1, no. 1, pp. 56–67, 1996.

[6] H. S. Lee and M. Tomizuka, "Robust motion controller design for high-accuracy positioning systems," *IEEE Transactions on Industrial Electronics*, vol. 43, no. 1, pp. 48–55, 1996.

[7] X. Jinbang, W. Wenyu, S. Anwen, and Z. Yu, "Detection and reduction of middle frequency resonance for an industrial servo," *Control Engineering Practice*, vol. 21, no. 7, pp. 899–907, 2013.

[8] G. Zhang and J. Furusho, "Speed control of two-inertia system by pi/pid control," *IEEE Transactions on Industrial Electronics*, vol. 47, no. 3, pp. 603–609, 2000.

[9] K. Szabat and T. Orlowska-Kowalska, "Vibration suppression in a two-mass drive system using pi speed controller and additional feedbacks—comparative study," *IEEE Transactions on Industrial Electronics*, vol. 54, no. 2, pp. 1193–1206, 2007.

[10] K. Sugiura and Y. Hori, "Vibration suppression in 2- and 3-mass system based on the feedback of imperfect derivative of the estimated torsional torque," *IEEE Transactions on Industrial Electronics*, vol. 43, no. 1, pp. 56–64, 1996.

[11] J. Kang, S. Chen, and X. Di, "Online detection and suppression of mechanical resonance for servo system," in *2012 Third International Conference on Intelligent Control and Information Processing*, pp. 16–21, 2012.

[12] W. Bahn, T.-I. Kim, S.-H. Lee, and D.-I. D. Cho, "Resonant frequency estimation for adaptive notch filters in industrial servo systems," *Mechatronics*, vol. 41, pp. 45–57, 2017.

[13] Y. Chen, M. Yang, J. Long, K. Hu, D. Xu, and F. Blaabjerg, "Analysis of oscillation frequency deviation in elastic coupling digital drive system and robust notch filter strategy," *IEEE Transactions on Industrial Electronics*, vol. 66, no. 1, pp. 90–101, 2019.

[14] W. Bolton, *Instrumentation and Control Systems*. Elsevier Science & Technology Books, 2004.